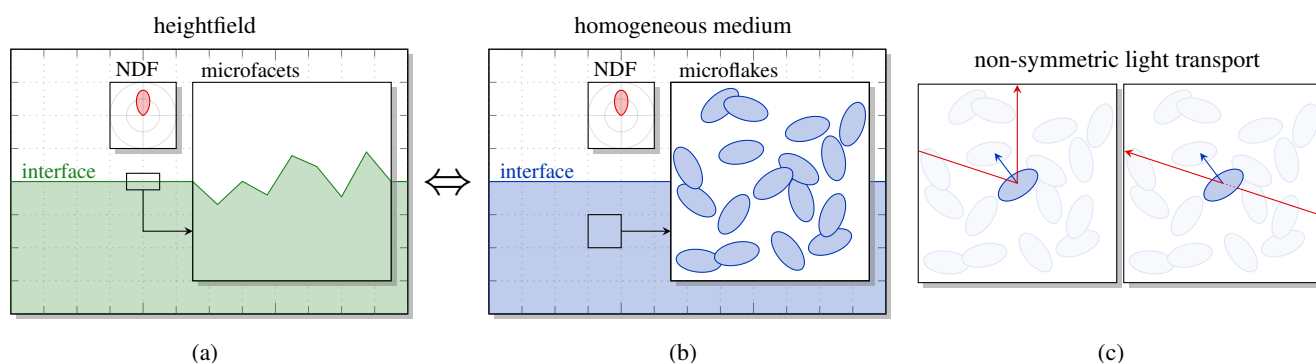


# Additional Progress Towards the Unification of Microfacet and Microflake Theories

Jonathan Dupuy  
Unity Technologies

Eric Heitz  
Unity Technologies

Eugene d'Eon  
8i



**Figure 1:** We show that light transport due to (a) a rough microfacet surface is the same as the light transport due to (b) a semi-infinite homogeneous microflake volume consisting of (c) non-symmetric microflakes that are reflective on one side and transparent on the other side, which have the same NDF as (a).

## Abstract

We study the links between microfacet and microflake theories from the perspective of linear transport theory. In doing so, we gain additional insights, find several simplifications and touch upon important open questions as well as possible paths forward in extending the unification of surface and volume scattering models. First, we introduce a semi-infinite homogeneous exponential-free-path medium that (a) produces exactly the same light transport as the Smith microsurface scattering model and the inhomogeneous Smith medium that was recently introduced by Heitz et al, and (b) allows us to rederive all the Smith masking and shadowing functions in a simple way. Second, we investigate in detail what new aspects of linear transport theory enable a volume to act like a rough surface. We show that this is mostly due to the use of non-symmetric distributions of normals and explore how the violation of this symmetry impacts light transport within the microflake volume without breaking global reciprocity. Finally, we argue that the surface profiles that would be consistent with very rough Smith microspheres have geometrically implausible shapes. To overcome this, we discuss an extension of Smith theory in the volume setting that includes NDFs on the entire sphere in order to produce a single unified reflectance model capable of describing everything from a smooth flat mirror all the way to a semi-infinite isotropically scattering medium with both low and high roughness regimes in between.

Categories and Subject Descriptors (according to ACM CCS): I.3.7 [Computer Graphics]: Three-Dimensional Graphics and Realism—Keywords: Microfacet theory, BRDF, BSDF, multiple scattering, anisotropic media

## 1. Introduction

This paper is a follow up to the recent work of Heitz et al. [HHdD16], who introduced a new approach to rough surface scattering. Where most previous parametric BSDF models consider only a single microsurface interaction, discarding the multiple scat-

tering and thereby losing energy, this new approach makes it practical to compute all orders of scattering from rough surfaces with conductive, dielectric or diffuse facets and for a variety of microfacet normal distribution functions (NDFs).

The model of Heitz et al. suggests that the scattering of light due

to rough surfaces is similar to the scattering of light due to participating media. In particular, Heitz et al. showed that light transport inside a new kind of heterogeneous microflake volume (anisotropic media) [JAM\*10] leads to the bidirectional scattering distribution function (BSDF) as predicted by microfacet theory [TS67] under the Smith shadowing hypothesis [Smi67]. It is the treatment of rough surface reflectance using volumes that we wish to investigate further here.

### 1.1. Surfaces as Volumes

Heitz et al. explored the properties of light transport on a Smith microsurface model and arrived at a formulation for light transport in a heterogeneous microflake volume. This is, perhaps, surprising at first because the two seemingly incompatible physical scenarios are very different. Indeed, classical participating media is not capable of accurately acting like a rough surface—a new phase function and a new non-symmetric microflake distribution are required. However, when these are suitably chosen, it is possible to bring the two models into complete agreement. It is this equivalence that makes it possible to stochastically evaluate the higher order interactions of a rough surface directly and accurately. The theoretical implications of this equivalence are worthy of further attention, especially in relation to linear transport theory [DM79] as a whole. The two key components that determine a heterogeneous microflake volume and that need to be investigated are the free path inside the medium and its phase function [JAM\*10]. New forms of both were required to derive a volume that acts like a rough surface.

**The Free path** The free path depends on the density function that describes how matter is concentrated throughout the volume; Heitz et al. use the height probability density function (PDF) of the rough surface they want to model for their BSDF derivation. In Section 4.1, we show that the first non-classical aspect of their model is that the anisotropic cross-sections of this matter density are non-symmetric to direction—the interaction probability when passing through a given location in the medium is not identical to the case where the direction is reversed. We explore this new aspect of volume transport, specifically the notion that subsurface violation of reciprocity nonetheless leads to reciprocal BSDFs.

**The Phase Function** The phase function is determined from combining a microflake NDF with a micro-BSDF that describes how light reacts after intersecting matter [JAM\*10, HCD15]; Heitz et al. use the microfacet NDF of the rough surface they want to model as the microflake NDF, and choose between conductor, dielectric or diffuse micro-BSDFs. In Section 4.3 we propose extending the microfacet NDFs to include distributions on the entire sphere. We discuss how moving beyond heightfields extends the utility of the approach to consider very rough and possibly semi-porous materials that are somewhat like a surface and somewhat like a volume.

### 1.2. Contributions and Overview

We dedicate the following sections to the investigation of the connection between rough-surface and volume scattering. Rather than relying on the theoretical framework of Heitz et al., which involves a heterogeneous microflake volume, we consider a semi-infinite,

homogeneous microflake volume. We show that the light transport that emerges from such media also maps to a rough surface, while being mathematically simpler than the model of Heitz et al. In addition, our derivations lead to new insights regarding the very nature of surfaces, which we discuss.

We first introduce our semi-infinite homogeneous microflake volume in Section 2 and discuss its scattering properties. Next, we show how to derive the model of Heitz et al. and show that it is equivalent to a microfacet BSDF with Smith shadowing in Section 3. Finally, we discuss specific properties of our model and raise several connections between rough microfacet surfaces and microflake volumes in Section 4; we hope our discussion will help in the derivation of a unified representation for matter that supports volumetric as well as surface like behaviors. In summary our contributions are:

- A new homogeneous derivation of a volume scattering approach to rough surface scattering that is simpler and more efficient to evaluate.
- A characterization of the change to previous volume scattering methods (non-symmetric cross-section) that enables surface-like behaviour.
- An analysis of reciprocity and its subsurface violation due to non-symmetric cross-section.
- A possible new approach for high roughness and semi-porous media using scattering methods analogous to Smith microsurface theory.

## 2. Semi-Infinite Homogeneous Microflake Volume

### 2.1. Volumetric Light Transport

In computer graphics, the light transport due to participating media is described by the steady radiative transfer equation (RTE) [JAM\*10]

$$\omega_1 \cdot \nabla L + \sigma_t L = S. \quad (1)$$

Here,  $\omega_1 \in S^2$  is the direction of radiation,  $L = L(\omega_1) \geq 0$  is the radiance,  $\sigma_t = \sigma_t(\omega_1) \geq 0$  is the medium's extinction coefficient, and  $S = S(\omega_1) \geq 0$  is the source term that accounts for the radiance emission of the medium and inscattering. Note that we suppressed the angular integral part of the RTE into the source term, i.e.,

$$S(\omega_1) = \sigma_s(\omega_1) \int_{S^2} f_p(\omega_1 \rightarrow \omega_2) L(\omega_2) d\omega_2 + L_e(\omega_1), \quad (2)$$

where  $L_e \geq 0$  is the radiance emitted by the medium,  $\sigma_s \geq 0$  is the medium's scattering coefficient, and  $f_p \geq 0$  is the medium's phase function. In order to derive the terms  $\sigma_t$ ,  $\sigma_s$ , and  $f_p$ , we need to fix the geometric properties of our microflake volume.

### 2.2. Semi-infinite Homogeneous Microflake Volume

**Medium Extent** We consider a semi-infinite homogeneous microflake volume, whose interface is located at height  $z = 0$ ; Figure 2 shows the geometry of such a volume. The matter density distribution function  $\rho = \rho(\mathbf{r}) \geq 0$ ,  $\mathbf{r} \in \mathbb{R}^3$ , which is defined such that  $\rho(\mathbf{r}) d\mathbf{r}$  gives the number of flakes located within the volume

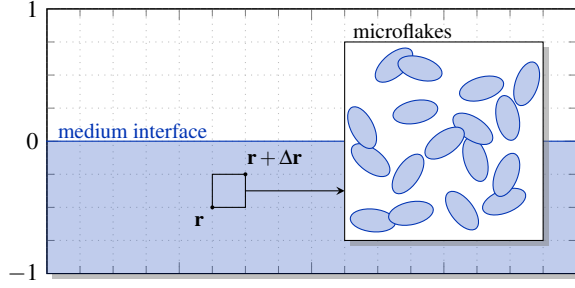


**Figure 2:** The semi-infinite homogeneous microflake volume.

$[\mathbf{r}, \mathbf{r} + d\mathbf{r}]$ , is

$$\rho(\mathbf{r}) = \begin{cases} 0 & \text{if } z_r > 0, \\ 1 & \text{otherwise.} \end{cases} \quad (3)$$

**Microflake Distribution** The microflake NDF  $D(\omega_m) \geq 0$  is defined such that  $D(\omega_m)d\omega_m$  gives the surface of flakes oriented towards the directions associated with the solid angle  $[\omega_m, \omega_m + d\omega_m]$ . Note that the NDF does not carry a spatial parameter  $\mathbf{r}$  as we follow the classic assumption that the directional statistics of the microflakes are independent from their location inside the volume. However, our NDF differs from previous Microflake NDFs as we do not enforce it to have a symmetric behavior, i.e.,  $D(\omega_m) \neq D(-\omega_m)$ . As we will discuss later, this form of NDF asymmetry is one of the key differences between microflake volumes that result in surface-like and volume-like light transport.

**Microflake Projected Area** In addition to spatial independence, we also follow the other classic assumption that the microflakes are spatially uncorrelated with one another as in a Poisson process. Then, the microflake projected area  $\sigma(\omega_1) \geq 0$ , which gives the area of matter that is visible from direction  $\omega_1 \in S^2$ , satisfies [HDCD15]

$$\sigma(\omega_1) = \int_{S^2} \langle -\omega_1, \omega_m \rangle D(\omega_m) d\omega_m. \quad (4)$$

The microflake projected area is a key quantity for light transport. Note that whenever  $D$  is non-symmetric,  $\sigma$  is also non-symmetric by construction, i.e.,  $\sigma(\omega_1) \neq \sigma(-\omega_1)$ .

**Microflake BSDF** The BSDF  $f_{s,\mu} = f_{s,\mu}(\omega_m, \omega_i, \omega_o) \geq 0$  describes how light reacts after intersecting a microflake. We do not assume any specific micro BSDF in our derivation as it does not impact our results.

### 2.3. Terms for Volumetric Light Transport

We now derive the terms of Equation (1) from the geometric properties of our microflake volume.

**Phase Function** The phase function is a measure of the probability density distribution for a scattering process from the incident direction  $\omega_1$  into the direction  $\omega_2$ . For a microflake volume, the phase

function satisfies [HDCD15]

$$f_p(\omega_1 \rightarrow \omega_2) = \int_{S^2} f_{s,\mu}(\omega_m, -\omega_1, \omega_2) \langle \omega_2, \omega_m \rangle D_{\text{vis}}(\omega_m, \omega_1) d\omega_m, \quad (5)$$

where we use the notation  $\langle \omega_1, \omega_2 \rangle$  to denote a dot product clamped to zero if it is negative and  $D_{\text{vis}} \geq 0$  is the distribution of visible microflake normals (VNDF), which is defined as

$$D_{\text{vis}}(\omega_m, \omega_1) = \frac{\langle -\omega_1, \omega_m \rangle D(\omega_m)}{\sigma(\omega_1)}. \quad (6)$$

Note that it is the microflake BSDF that determines how light reacts after intersecting a microflake and, as such, completely determines the category of the material, e.g., conductor, dielectric, etc.

**Scattering Coefficient** Assuming that the microflakes carry the same material albedo  $a \geq 0$ , the scattering coefficient is [JAM\*10]

$$\sigma_s = a\sigma_r. \quad (7)$$

**Extinction Coefficient** In a microflake volume, the extinction coefficient is the product of the density and the projected area of the microflakes onto the ray direction. Since the matter density distribution  $\rho$  is constant inside our medium, it follows that the extinction coefficient only depends on the projected area, i.e.,

$$\begin{aligned} \sigma_r &= \rho\sigma \\ &= \sigma. \end{aligned} \quad (8)$$

**Free-Path PDF** The free path describes how far light is expected to travel through our volume without intersecting a microflake. The geometric configuration of our microflake volume satisfies the Beer-Lambert law, which stipulates that any free path of length  $\ell \geq 0$  that travels towards direction  $\omega_r$ , has the exponential probability density function (PDF)

$$\begin{aligned} p(\ell) &= \sigma_r \exp(-\sigma_r \ell) \\ &= \sigma \exp(-\sigma \ell). \end{aligned} \quad (9)$$

Note that the free path PDF  $p$  depends on  $\omega_r$ , but we omit it for clarity. It follows that a free path length  $\ell$  can be retrieved by inverse transform sampling a uniform random number  $\mathcal{U} \in [0, 1]$  [RSK08]

$$\begin{aligned} \ell &= -\frac{1}{\sigma_r} \log(1 - \mathcal{U}) \\ &= -\frac{1}{\sigma} \log(1 - \mathcal{U}). \end{aligned} \quad (10)$$

**Volumetric Attenuation** The distance between two points at respective locations  $\mathbf{r}_1$  and  $\mathbf{r}_2$  connected by a ray traveling towards direction  $\omega_1$  is  $\ell = |\mathbf{r}_1 - \mathbf{r}_2|$ . The volumetric attenuation along this segment is the integral

$$\begin{aligned} V(\mathbf{r}_1 \xrightarrow{\omega_1} \mathbf{r}_2) &= 1 - \int_0^\ell p(\ell') d\ell' \\ &= \exp(-\sigma_r(\omega_1) \ell) \\ &= \exp(-\sigma(\omega_1) \ell). \end{aligned} \quad (11)$$

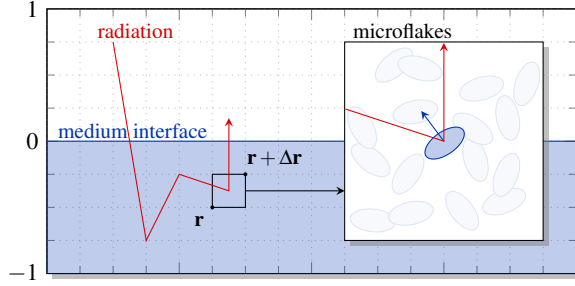


**Figure 3:** The emerging transport. *The Smith BSDF emerges from the light transport within the semi-infinite homogeneous microflake volume.*

## 2.4. Volumetric Light Transport Properties

In the general case, the light transport produced by our volume as described in Equation (1) has to be solved numerically. Typically, this is done with a Monte Carlo simulation, which, intuitively, consists in averaging the behavior of light paths simulated explicitly inside the microflake volume; Figure 3 illustrates this idea. The simulation requires the stochastic generation of light paths, i.e., Equation (10), as well as the volumetric attenuation due to the media between two points, i.e., Equation (11). Within the volume, all light paths depend also on the volume's phase function, i.e., Equation (5). We do not discuss this particular simulation here, as this feature is not relevant to the following discussion; we refer the reader to the work of Heitz et al. [HHdD16] for more information. Rather, we show in Section 3 that the classic Smith masking and shadowing functions can be derived from our model.

## 3. Derivation of the Smith Shadowing Functions

### 3.1. Mapping our Media to Smith Microsurfaces

The light transport in both media is identical because the single-scattering albedo and phase function do not depend on depth (this is analogous to the optical-depth parameterization of plane-parallel media in classical transport theory).

**Smith Density Model** The elevations  $\zeta \in \mathbb{R}$  of a microsurface are distributed according to the distribution of heights  $P_1(\zeta)$ . It is a probability density function (PDF) and we denote the cumulative distribution function (CDF) of heights as  $C_1(\zeta)$  and the inverse CDF as  $C_1^{-1}$ . The density of the microflake volume associated with a Smith microsurface derived by Heitz et al. is [HHdD16, Eq. (19)]

$$\rho_{\text{Smith}}(\zeta) = \frac{P_1(\zeta)}{C_1(\zeta)}. \quad (12)$$

**Mapping to Homogeneous Media** We can map the heights  $z$  of a semi-infinite homogeneous medium to the heights of a Smith microsurface  $\zeta$  through the relations

$$z = \log[C_1(\zeta)] \quad (13)$$

$$\zeta = C_1^{-1}[\exp(z)]. \quad (14)$$

Our mapping produces the same medium density since

$$\begin{aligned} \rho_{\text{Smith}}(\zeta) &= \rho(z) \frac{\partial z}{\partial \zeta} \\ &= \frac{P_1(\zeta)}{C_1(\zeta)} \end{aligned} \quad (15)$$

is the expected Smith density of Equation (12); Figure 4 illustrates the geometry of our mapping.

**Simulating Points inside the Volume** Simulating points inside our volume is important for the derivation of the Smith masking-shadowing functions [HHdD16]. In order to create such a point, we can first simulate a Smith microsurface height  $\zeta$  through inverse transform sampling a random uniform variate  $\mathcal{U} \in [0, 1)$  and then applying Equation (14) to map it to our medium, which gives

$$\begin{aligned} z &= \log[C_1(\zeta)] \\ &= \log\{C_1[C_1^{-1}(\mathcal{U})]\} \\ &= \log(\mathcal{U}). \end{aligned} \quad (16)$$

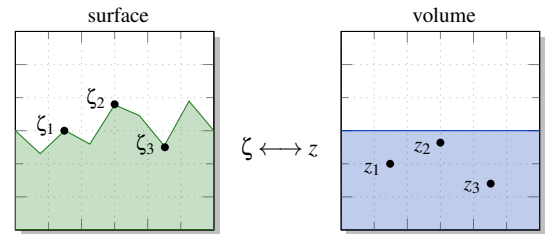


**Figure 4:** Mapping the semi-infinite medium to a Smith microsurface.

### 3.2. Derivation of the Smith Functions

**Heightfield NDF** The Smith shadowing functions arise from exponential attenuation due to our microflake volume if the microflake NDF corresponds to a heightfield NDF. A heightfield NDF is a non-symmetric NDF in the sense that its values are nonnegative in a hemisphere  $\mathcal{H}^2 \subset S^2$  and 0 in the other. Moreover, it satisfies

$$\int_{S^2} D(\omega_m) \langle \omega_m, \omega_g \rangle d\omega_m = 1 \quad (17)$$

where  $\omega_g$  gives the orientation of  $\mathcal{H}^2$ .

**Smith Lambda Function** The Smith  $\Lambda$  function is associated with the projected area of heightfield NDFs through the relation [HHdD16, Eq. (21)]

$$\begin{aligned} \sigma(\omega_i) &= \int_{S^2} \langle -\omega_i, \omega_m \rangle D(\omega_m) d\omega_m \\ &= \Lambda(\omega_i) \cos \theta_i. \end{aligned} \quad (18)$$

Note that due to the non-symmetry of the heightfield NDF, we have [HHdD16, Eq. (22)]

$$\begin{aligned} \sigma(-\omega_i) &= \int_{S^2} \langle \omega_i, \omega_m \rangle D(\omega_m) d\omega_m \\ &= [1 + \Lambda(\omega_i)] \cos \theta_i. \end{aligned} \quad (19)$$

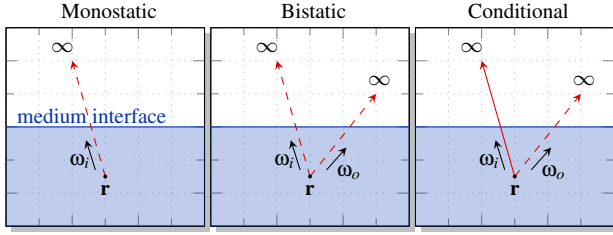


**Figure 5:** Geometry of the Smith shadowing functions. *Left:* The Smith masking function is the probability that a random point  $\mathbf{r}$  inside the volume is visible from outside in direction  $\omega_i$ . *Middle:* The Smith masking-shadowing function is the probability that a random point  $\mathbf{r}$  inside the volume is visible from outside from both directions  $\omega_i$  and  $\omega_o$ . *Right:* The conditional Smith shadowing term gives the conditional probability that a random point  $\mathbf{r}$  inside the volume is visible from outside from direction  $\omega_i$  given it is visible from outside from direction  $\omega_o$ .

**Smith Monostatic Shadowing** The Smith monostatic shadowing function, also known as the Smith masking term, is the probability that a random point inside the medium at height  $z$  is visible from the outside in direction  $\omega_i$

$$\begin{aligned} \mathbb{E}[V(\mathbf{r} \xrightarrow{\omega_i} \infty)] &= \int_0^1 V[\mathbf{r}(\mathcal{U}) \xrightarrow{\omega_i} \infty] d\mathcal{U} \\ &= \int_0^1 \exp\left[-|\log(\mathcal{U})| \frac{\sigma(\omega_i)}{\cos\theta_i}\right] d\mathcal{U} \\ &= \frac{1}{1 + \frac{\sigma(\omega_i)}{\cos\theta_i}} \\ &= \frac{1}{1 + \Lambda(\omega_i)}. \end{aligned} \quad (20)$$

Figure 5 shows the geometry of the Smith monostatic shadowing function in our microflake volume.

**Smith Bistatic Shadowing** The Smith bistatic shadowing function, also known as the Smith masking and shadowing term, is the probability that a random point inside the medium at height  $z$  is visible from both the outside directions  $\omega_i$  and  $\omega_o$

$$\begin{aligned} \mathbb{E}[V(\mathbf{r} \xrightarrow{\omega_i} \infty) V(\mathbf{r} \xrightarrow{\omega_o} \infty)] &= \int_0^1 V(\mathbf{r}(\mathcal{U}) \xrightarrow{\omega_i} \infty) V(\mathbf{r}(\mathcal{U}) \xrightarrow{\omega_o} \infty) d\mathcal{U} \\ &= \int_0^1 \exp\left\{-|\log(\mathcal{U})| \left[\frac{\sigma(\omega_i)}{\cos\theta_i} + \frac{\sigma(\omega_o)}{\cos\theta_o}\right]\right\} d\mathcal{U} \\ &= \frac{1}{1 + \frac{\sigma(\omega_i)}{\cos\theta_i} + \frac{\sigma(\omega_o)}{\cos\theta_o}} \\ &= \frac{1}{1 + \Lambda(\omega_i) + \Lambda(\omega_o)}, \end{aligned} \quad (21)$$

Figure 5 shows the geometry of the Smith bistatic shadowing function in our microflake volume.

**Conditional Smith Shadowing** The conditional Smith shadowing function, also known as the Smith shadowing given masking term, is the probability that a random point  $\mathbf{r}$  inside the medium is visible

from the outside in direction  $\omega_o$ . It differs from the Smith monostatic shadowing function in the sense that  $\mathbf{r}$  is not generated from Equation (16) but from a path originating from direction  $\omega_i$

$$\begin{aligned} \mathbb{E}[V(\mathbf{r} \xrightarrow{\omega_o} \infty) | V(\mathbf{r} \xrightarrow{\omega_i} \infty)] &= \int_0^1 \exp\left[-|\log(\mathcal{U})| \frac{\cos\theta_i}{\sigma(\omega_i)} \frac{\sigma(\omega_o)}{\cos\theta_o}\right] d\mathcal{U} \\ &= \frac{1}{1 + \frac{\cos\theta_i}{\sigma(\omega_i)} \frac{\sigma(\omega_o)}{\cos\theta_o}} \\ &= \frac{1 + \Lambda(\omega_i)}{1 + \Lambda(\omega_i) + \Lambda(\omega_o)}. \end{aligned} \quad (22)$$

Figure 5 shows the geometry of the Smith conditional shadowing function in our microflake volume.

## 4. Open Questions

### 4.1. The Reciprocity with Non-Symmetric NDFs

In this section we show that the non-symmetry of the NDF is what allows for surface-like transport, but at the same time breaks the reciprocity inside the volume.

**Mono-sided Flakes** As shown in Figure 6, if the NDF is non-symmetric, the light transport is non-reciprocal: the light is blocked by the existing side of the facet, but can go through the other side.

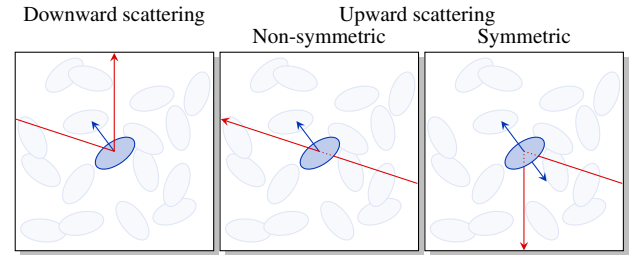


**Figure 6:** Mono-sided flakes. *If the NDF is non-symmetric, the flakes are mono-sided: the light is blocked by the existing side of the facet, but can go through the other side.*

**Surface-like Transport with Mono-side Flakes** It is precisely because the NDF is non-symmetric that the volumetric transport is able to mimic surface-like transport. For instance, Figure 7 shows the transport occurring on a flat specular microsurface and in a volume with the same NDF. Thanks to the non-reciprocal flakes, the light is able to escape the volume after the first bounce and the light transport is the same. If the flakes were double-sided the light would intersect the flakes multiple times before leaving the volume and the transport would be modified.

**Non-Reciprocal Transport** In general the visibility is non-reciprocal

$$V(\mathbf{r}_1 \xrightarrow{\omega_1} \mathbf{r}_2) \neq V(\mathbf{r}_2 \xrightarrow{-\omega_1} \mathbf{r}_1) \quad (23)$$

as illustrated in Figure 8.

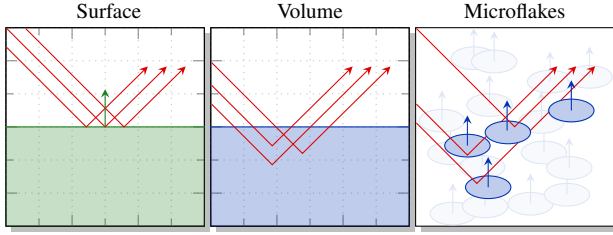


**Figure 7:** Surface-like transport in our microflake volume. Thanks to the mono-sided flakes, the light intersects the flakes only on the upper side, and the light transport in the volume matches the light transport on a surface.

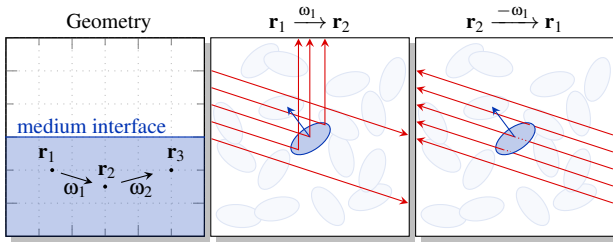


**Figure 8:** Non-reciprocity of the light transport. Because of the mono-sided flakes, the projected area is different for two opposite directions. Hence, the visibility of point  $\mathbf{r}_1$  for point  $\mathbf{r}_2$  is different from the visibility of point  $\mathbf{r}_2$  for point  $\mathbf{r}_1$ . However, in the case where the starting and final heights are the same, the light transport is reciprocal, e.g., from point  $\mathbf{r}_1$  to point  $\mathbf{r}_3$  through point  $\mathbf{r}_2$ .

**Globally Reciprocal** However, if the starting point is at the same height as the last point (Figure 8), the attenuation along the path is the same in both directions:

$$V(\mathbf{r}_1 \xrightarrow{\omega_1} \mathbf{r}_2)V(\mathbf{r}_2 \xrightarrow{\omega_2} \mathbf{r}_3) = V(\mathbf{r}_3 \xrightarrow{-\omega_2} \mathbf{r}_2)V(\mathbf{r}_2 \xrightarrow{-\omega_1} \mathbf{r}_1) \quad (24)$$

Hence, the attenuation along a path that starts from outside and finishes outside (i.e. above 0) is the same in both directions. This is why the BSDF emerging from the transport in the semi-infinite medium is reciprocal.

**Open Questions** We know that if  $D$  is a non-symmetric height-field microfacet NDF, the emerging transport is reciprocal and this is also the case if  $D$  is a symmetric microflake NDF. Can we determine the exact set of NDFs  $D$  such that the emerging transport is reciprocal?

Is it possible to model rough-surface scattering with another interpretation than “mono-sided flakes” due to non-symmetric NDFs? In microfacet theory, with the surface interpretation, the NDF is non-symmetric and the flakes are mono-sided because the ray can only intersect the facets that are on the same side of the surface, i.e., the other side of the surface (and of the flakes) cannot be intersected. This knowledge (the ray is on one side of the surface) is what breaks the reciprocity of the light transport inside the medium if the end points of a path are not at the same height. A point above the medium is obviously above the surface. However, the lower the point is inside the medium, the less likely that it is still above the surface. Hence, the lowest point of a path is the one that carries the most information. Intuitively, the information loss/gain when the

depth within the medium changes is what breaks the reciprocity of the light transport. This is also why if the end points of a path are at the same height, the light transport remains reciprocal. We believe that the existence of mono-sided flakes in our model is a side effect of an additional information that remains to be modeled properly, for instance with a conditional probability. This could yield a generalized formulation of the reciprocity inside the medium.

Given a general microflake volume represented as voxels, such as the assets of Jakob et al. [JAM\*10], is it valid to have “surface-like voxels” that represent non-symmetric NDFs? Or can non-symmetric NDFs be used only with the semi-infinite medium model? It is possible that a new conditional model as discussed in the previous question (with knowledge that the ray is inside/outside the surface) could yield a generalized and valid light transport formulation and overcome the semi-infinite medium limitation.

## 4.2. Perspectives from Linear Transport Theory

**Scattering Inside the Medium** An important aspect of Heitz et al.’s approach is that the multiple-scattering component of the BSDF must be evaluated stochastically. While this is unusual for most parametric microfacet BSDFs, it is very common for BSDFs derived from subsurface-scattering models. Such derivations assume the lateral displacements in the medium are negligible and average them away or, equivalently, consider uniform illumination by parallel rays. This *plane-parallel* analysis in transport theory is very common and much simpler than the derivation of full BSS-RDFs.

**Connection to Results of Linear Transport Theory** For example, in the simple case of an isotropically scattering semi-infinite medium with single-scattering albedo  $a$ , the single-scattering BRDF is known from Chandrasekhar [Cha60] and is simply

$$f_1(\omega_i, \omega_o) = \frac{a}{4\pi \cos \theta_i + \cos \theta_o}. \quad (25)$$

We note that our model naturally includes such an isotropic medium with an isotropic phase function. Consider, for example, isotropic scattering, which arises from mirror reflection from an isotropic NDF (a constant). As a proof, we derive this single-scattering BRDF using the methods developed in the previous sections. The cosine-weighted single-scattering BRDF of a semi-infinite medium is the phase function  $f_p(\omega_i, \omega_o)$  multiplied by the shadowing-given-masking function  $\mathbb{E}[V(\mathbf{r} \xrightarrow{\omega_2} \infty) | V(\infty \xrightarrow{\omega_1} \mathbf{r})]$  of Equation (22):

$$\begin{aligned} & f_1(\omega_i, \omega_o) \cos \theta_o \\ &= f_p(\omega_1 \rightarrow \omega_2) \mathbb{E}[V(\mathbf{r} \xrightarrow{\omega_2} \infty) | V(\infty \xrightarrow{\omega_1} \mathbf{r})], \end{aligned} \quad (26)$$

In an isotropic medium the isotropic phase function of albedo  $a$  is

$$f_p(\omega_1 \rightarrow \omega_2) = \frac{a}{4\pi}, \quad (27)$$

and since the projected area is constant ( $\sigma = 1$ ), the shadowing-given-masking function Equation (22) simplifies to

$$\mathbb{E}[V(\mathbf{r} \xrightarrow{\omega_2} \infty) | V(\infty \xrightarrow{\omega_1} \mathbf{r})] = \frac{1}{1 + \frac{\cos \theta_o}{\cos \theta_i}}. \quad (28)$$

With these simplifications, the cosine-weighted single-scattering BRDF of Equation (26) is

$$f_1(\omega_i, \omega_o) \cos \theta_o = \frac{a}{4\pi} \frac{1}{1 + \frac{\cos \theta_o}{\cos \theta_i}}, \quad (29)$$

and the BRDF is the result of Equation (25).

**Plane-Parallel Analysis** The plane-parallel analysis makes it possible to derive the complete BRDF of the isotropic medium, which is known as

$$f_r(\omega_i, \omega_o) = \frac{a}{4\pi} \frac{H(\cos \theta_i)H(\cos \theta_o)}{\cos \theta_i + \cos \theta_o} \quad (30)$$

where  $H$  is Chandrasekhar's function, the solution to an integral equation [Cha60]. A closed-form expression was derived for  $H$  [SW59],

$$H(u = \cos \theta) = \exp\left(-\frac{u}{\pi} \int_0^{\frac{\pi}{2}} \frac{\log(1 - t a \cot(t))}{u^2 \sin^2(t) + \cos^2(t)} dt\right). \quad (31)$$

**Open Questions** Chandrasekhar was able to derive this result using a principle of invariance, avoiding the need for stochastic (random walk) evaluation of the full BRDF. His result can also be arrived at using the alternative singular-eigenfunction [MK73] or Wiener-Hopf [Wil73] methods. These approaches demonstrate the power of deterministic analysis of the transport equation. Can they provide similar utility for rough-surface scattering? Toward this end, the singular-eigenfunction method has been extended to plane-parallel transport in anisotropic media [FG07]. In the anisotropic media case, the discrete eigenvalues no longer occur in conjugate pairs and the rigorous asymptotic diffusion term satisfies an equation that includes an advective flow term [CW92]. An interesting follow up to this work would be to investigate the inclusion of non-symmetric cross-sections to support rough-surface scattering such as in microfacet theory.

### 4.3. Extension to Spherical NDFs

In this section we consider an extension of the model of Heitz et al. to include NDFs on the entire sphere in order to exhibit different high roughness behavior and new reflectance behaviors that might better approximate semi-porous media.

**The Problem with High Roughness** A fundamental limitation of heightfield rough-surface models is that for very high roughness levels, the surface profiles consistent with those NDFs are unreasonably spiky (Figure 9). The Beckmann NDF, for example, corresponds to quite spiky surfaces past a roughness of about 0.8.

**Isotropic Scattering as a Limit of Infinite Roughness** The relationship between rough surface and volume scattering offers an alternative approach to high roughness scattering by considering that an isotropically scattering semi-infinite medium is, by some definition, the roughest surface model possible. Further, it happens that far-field reflectance from a spherical mirror produces isotropic scattering. These two insights lead us to propose an extension of the model presented in this paper to permit NDFs on the full sphere. We propose a comprehensive rough surface scattering model with an NDF that:

- Is a dirac delta of the up direction for roughness  $m = 0$  (producing a flat mirror)
- Is asymptotic to the Beckmann NDF for low  $m$
- Smoothly extends into the constant NDF on the entire sphere as  $m \rightarrow \infty$

Physically, this would correspond to surfaces much like Beckmann Gaussian heightfields, but as roughness increases they become semi-porous and eventually turn into a sea of mirror spheres. Figure 12 shows a possible adequate behavior for a family of spherical NDF smoothly morphing from a rough-surface profile to an isotropic volume profile. Indeed, as we show in Section 4.2, our model extends naturally to include an NDF  $D$  on the entire sphere and eventually to Chandrasekhar's isotropic-scattering model.

**Open Questions** Additional work is required to investigate the feasibility of analytically sampling the visible distribution of normals with such an NDF, which may present a significant challenge, given the complexity of doing so for Beckmann and GGX [Hd14]. Success would produce a single reflection model that could span from mirror, rough conductor, semi-porous high roughness conductor and bridge the gap from surface to volume and into Chandrasekhar's BRDF for the isotropic semi-infinite medium. Such reflectance distributions might prove useful for better describing materials in the high reflectance regime as well as possibly predict aggregate reflectance for volumetric level-of-detail simplification schemes for light transport.

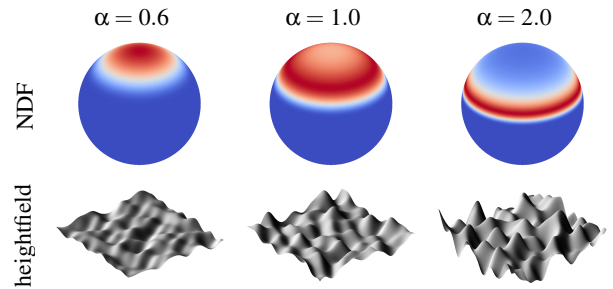


Figure 11: Beckmann heightfields.

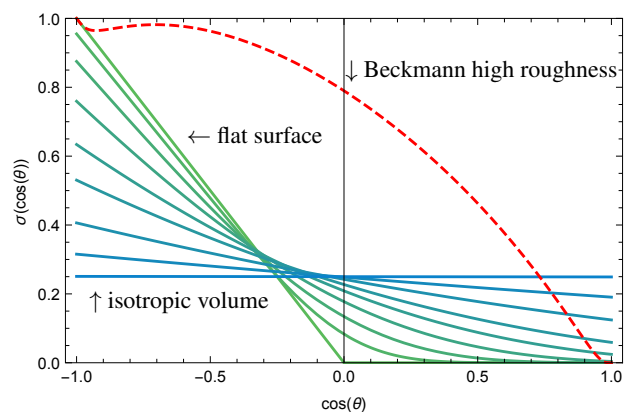
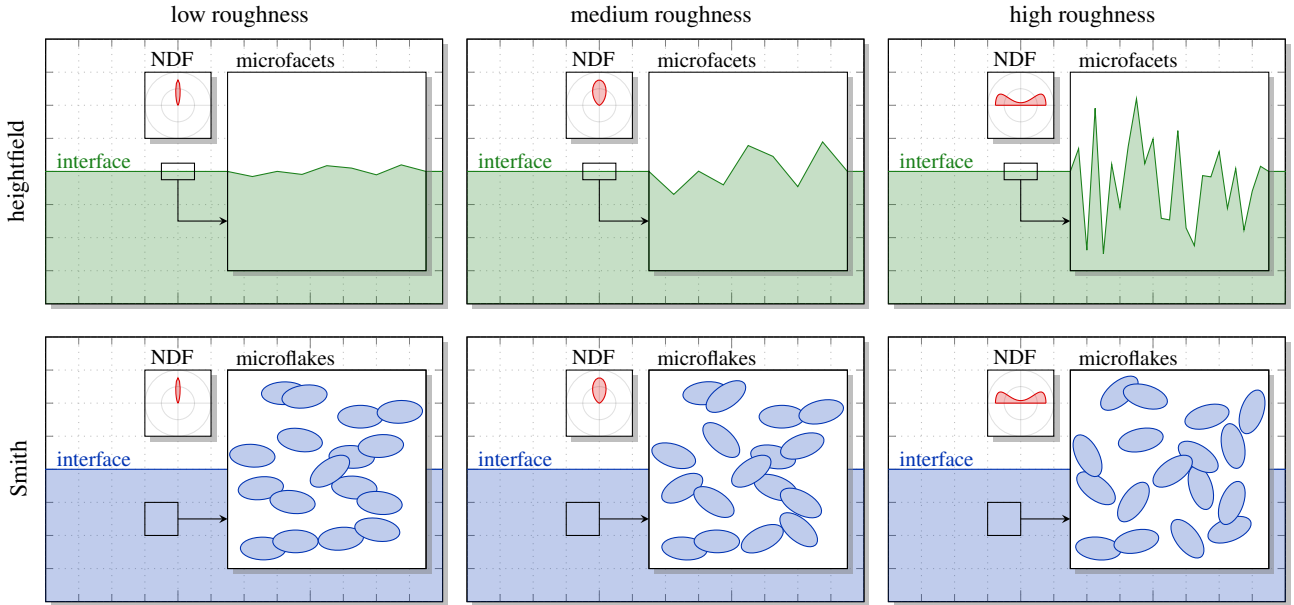
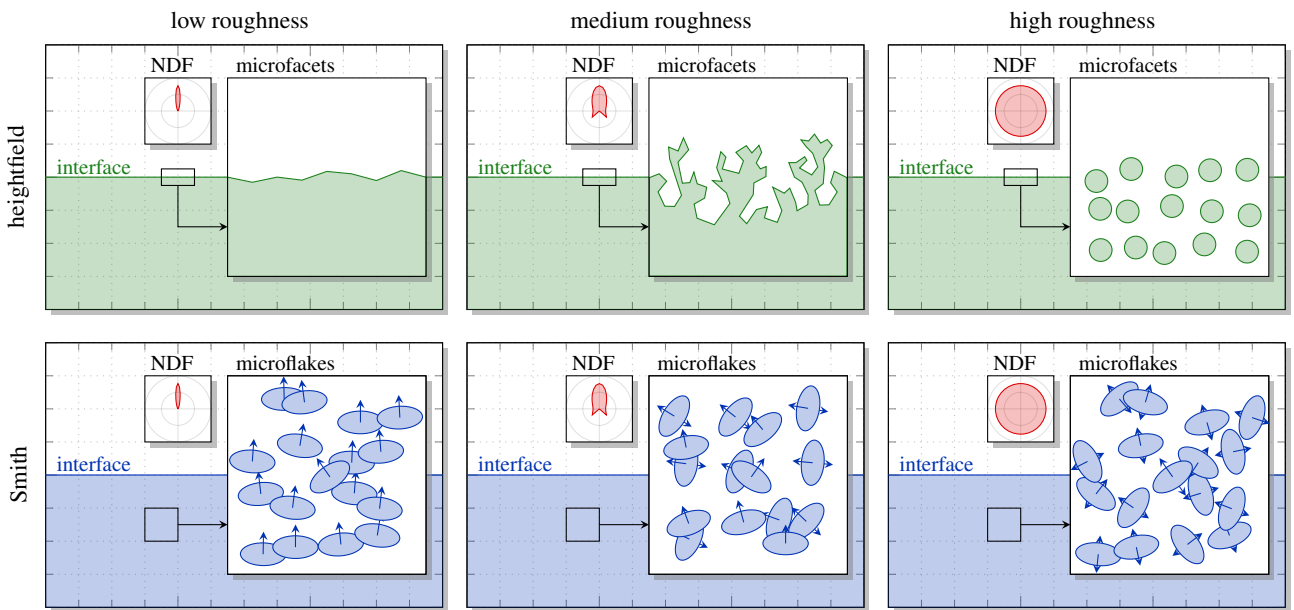


Figure 12: Spherical NDF family of scattering cross-sections  $\sigma(\cos \theta)$ .



**Figure 9:** Classic parameterization of microfacet distribution. With common hemispherical microfacet distributions, the roughness parameter controls the vertical scaling of the surface. Hence, a very high roughness is associated with spiky unrealistic surfaces.



**Figure 10:** Alternate NDF parameterization. One could use an NDF that allows for transition between different shapes: hemispherical (heightfield-like transport), non-hemispherical (non-heightfield surface), and constant (pure volumetric transport).



## 5. Conclusion

We have revisited the relationship between rough surface and volume scattering. We have derived a new homogeneous semi-infinite microflake model with asymmetric flakes that exactly produces multiple reflectance from Smith microspheres, reducing the complexity of the previous inhomogeneous derivations and strengthening the connections between surface and volume scattering. We uncovered a subsurface violation of reciprocity that arises from asymmetric microflake cross-sections that is required to make the volume behave like a surface and showed how an equal-height reciprocity ensures that the full model is reciprocal. We also proposed an extension of these methods to include NDFs on the entire sphere to encompass new reflectance behaviors, such as very rough and semi-porous media and to bridge the gap between surface and volume scattering in a single model.

## References

- [Cha60] CHANDRASEKHAR S.: *Radiative Transfer*. Dover, 1960. 6, 7
- [CW92] CASSELL J., WILLIAMS M.: Discrete eigenvalues of the one-speed transport equation for asymmetric scattering. *Annals of Nuclear Energy* 19, 7 (1992), 403–407. 7
- [DM79] DUDERSTADT J., MARTIN W.: *Transport theory*. Wiley-Interscience, 1979. 2
- [FG07] FURFARO R., GANAPOL B.: Spectral Theory for Photon Transport in Dense Vegetation Media: Caseology for the Canopy Equation. *Transport Theory and Statistical Physics* 36, 1 (2007), 107–135. 7
- [Hd14] HEITZ E., D'EON E.: Importance sampling microfacet-based BSDFs using the distribution of visible normals. In *Proc. Eurographics Symposium on Rendering* (2014), pp. 103–112. 7
- [HDCD15] HEITZ E., DUPUY J., CRASSIN C., DACHSBACHER C.: The SGGX microflake distribution. *ACM Transactions on Graphics (Proc. SIGGRAPH)* 34, 4 (2015), 48:1–48:11. 2, 3
- [Hei14] HEITZ E.: Understanding the masking-shadowing function in microfacet-based BRDFs. *Journal of Computer Graphics Techniques* 3, 2 (2014), 32–91.
- [HHdD16] HEITZ E., HANIKA J., D'EON E., DACHSBACHER C.: Multiple-scattering microfacet BSDFs with the Smith model. *Conditionally accepted at SIGGRAPH* (2016). 1, 4
- [JAM\*10] JAKOB W., ARBREE A., MOON J. T., BALA K., MARSCHNER S.: A radiative transfer framework for rendering materials with anisotropic structure. *ACM Transactions on Graphics (Proc. SIGGRAPH)* 29, 4 (2010), 53:1–53:13. 2, 3, 6
- [JdJM14] JAKOB W., D'EON E., JAKOB O., MARSCHNER S.: A comprehensive framework for rendering layered materials. *ACM Transactions on Graphics (Proc. SIGGRAPH)* 33, 4 (2014), 118:1–118:14.
- [MK73] MCCORMICK N., KUŠČER I.: Singular eigenfunction expansions in neutron transport theory. *Advances in Nuclear Science and Technology* 7 (1973), 181–282. 7
- [RSK08] RAAB M., SEIBERT D., KELLER A.: Unbiased global illumination with participating media. In *Monte Carlo and Quasi-Monte Carlo Methods 2006* (2008), pp. 591–606. 3
- [Smi67] SMITH B.: Geometrical shadowing of a random rough surface. *IEEE Transactions on Antennas and Propagation* 15 (1967), 668–671. 2
- [SW59] STIBBS D., WEIR R.: On the H-functions for isotropic scattering. *Monthly Notices of the Royal Astronomical Society* 119 (1959), 512. 7
- [TS67] TORRANCE K. E., SPARROW E. M.: Theory for off-specular reflection from roughened surfaces. *Journal of the Optical Society of America (JOSA)* 57, 9 (1967), 1105–1112. 2
- [Wil73] WILLIAMS M.: The wiener-hopf technique: An alternative to the singular eigenfunction method. *Advances in Nuclear Science and Technology* 7 (1973), 283–327. 7